Radiation Exposure to Patients in a Multicenter Coronary Angiography Trial (CORE 64)

Jacob Geleijns[1]
Raoul M. S. Joemai[1]
Marc Dewey[2]
Albert de Roos[1]
Maria Zankl[3]
Alfonso Calzado Cantera[4]
Marçal Salvadó Artells[5]

Keywords: coronary angiography, coronary CT angiography, dosimetry methods, radiation dosage

DOI:10.2214/AJR.09.3983

Received November 17, 2009; accepted after revision September 10, 2010.

M. Dewey has been awarded research grants from the European Regional Development Fund, the German Heart Foundation/German Foundation of Heart Research, GE Healthcare (Amersham), Bracco, Guerbet, and Toshiba Medical Systems. He is a member of the speakers' bureau for Toshiba Medical Systems, Guerbet, Cardiac MR Academy Berlin, and Bayer Schering and is a consultant to Guerbet. He receives royalties from Springer for his 2008 book titled *Coronary CT Angiography*. He has institutional master research agreements with Siemens Healthcare, Philips Healthcare, and Toshiba Medical Systems.

[1]Department of Radiology, Leiden University Medical Center, Albinusdreef 2, 2333 ZA Leiden, The Netherlands. Address correspondence to J. Geleijns (K.Geleijns@lumc.nl).

[2]Department of Radiology, University Hospital Charité, Hospital Charitéplatz, Berlin, Germany.

[3]Helmholtz Zentrum München, German Research Center for Environmental Health, Neuherberg, Germany.

[4]Department of Medical Physics, Complutense University, Ciudad Universitaria, Madrid, Spain.

[5]Faculty of Medicine and Health Sciences, Rovira i Virgili University, Reus, Spain.

AJR 2011; 196:1126–1132

0361–803X/11/1965–1126

OBJECTIVE. The objective of this study was to assess the exposure of patients to radiation for the cardiac CT acquisition protocol of the multicenter Coronary Artery Evaluation Using 64-Row Multidetector Computed Tomography Angiography (CORE 64) trial.

MATERIALS AND METHODS. An algorithm for patient dose assessment with Monte Carlo dosimetry was developed for the Aquilion 64-MDCT scanner. During the CORE 64 study, different acquisition protocols were used depending on patient size and sex; therefore, six patient models were constructed representing three men and three women in the categories of small, normal size, and obese. Organ dose and effective dose resulting from the cardiac CT protocol were assessed for these six patient models.

RESULTS. The average effective dose for coronary CT angiography (CTA) calculated according to Report 103 of the International Commission on Radiological Protection (ICRP) is 19 mSv (range, 16–26 mSv). The average effective dose for the whole cardiac CT protocol including CT scanograms, bolus tracking, and calcium scoring is slightly higher—22 mSv (range, 18–30 mSv). An average conversion factor for the calculation of effective dose from dose-length product of 0.030 mSv/mGy · cm was derived for coronary CTA.

CONCLUSION. The current methods of assessing patient dose are not well suited for cardiac CT acquisitions, and published effective dose values tend to underestimate effective dose. The effective dose of cardiac CT is approximately 25% higher when assessed according to the preferred ICRP Report 103 compared with ICRP Report 60. Underestimation of effective dose by 43% or 53% occurs in coronary CTA according to ICRP Report 103 when a conversion factor (E / DLP, where E is effective dose and DLP is dose-length product) for general chest CT of 0.017 or 0.014 mSv/mGy · cm, respectively, is used instead of 0.030 mSv/mGy · cm.

Coronary CT angiography (CTA) is widely used to rule out coronary artery disease. The diagnostic performance of coronary CTA improved significantly with the introduction of 32- and 64-MDCT scanners compared with the preceding systems with 4- and 16-MDCT scanners [1, 2]. The results of a multicenter trial with the participation of nine sites worldwide on cardiac 64-MDCT have been reported [3]: The study is titled the "Coronary Artery Evaluation Using 64-Row Multidetector Computed Tomography Angiography Study" and is referred to as the "CORE 64 study" [3]. The objective of the clinical CORE 64 study was to evaluate the diagnostic accuracy of 64-MDCT for identifying coronary artery stenosis. The study presented here reports on the assessment of patient dose. Dose assessment is particularly relevant for cardiac CT because it is increasingly used in patient groups with various risk profiles [4, 5].

The CT acquisitions that were performed according to the CORE 64 acquisition protocol during one cardiac CT examination included two CT scanograms, calcium scoring, region-of-interest (ROI) planning, bolus tracking, and coronary CTA. Existing dosimetric methods did not allow appropriate assessment of organ dose and effective dose because they did not permit us to take into account accurately the characteristics of the Aquilion 64 CT scanner (Toshiba Medical Systems), they did not facilitate taking into account different patient sizes, and they did not allow dose assessment for CT scanograms.

The purpose of this study was to assess patient dose for the CORE 64 cardiac CT acquisition protocol taking into account the

characteristics of the CT scanner (Aquilion 64) and patient size and sex. Our findings were compared with other reported values of effective dose in coronary CTA.

Materials and Methods

A comprehensive assessment of patient dose was completed for examinations performed according to the cardiac CT protocol of the CORE 64 study. During the trial, patients were positioned on a CT table with an offset to the right so that the position of the heart coincided with the axis of rotation. Each examination started with two CT scanograms, one frontal and one lateral (beam collimation, 2 mm; tube current, 50 mA; table speed, 100 mm/s). Next, unenhanced prospective heart rate–triggered axial scanning of the heart was performed for calcium scoring (slice thickness, 3 mm; tube current, 50 mA; 0.25-second partial rotation). In preparation of coronary CTA, a 2-mm thin axial slice was acquired for planning the appropriate ROI for contrast bolus tracking within the descending aorta (tube current, 50 mA; rotation time, 0.4 second). Next, a dynamic scan was obtained (slice thickness, 2 mm; rotation time, 0.4 second; scan time, ≈ 10 seconds) to detect when contrast enhancement exceeded the preset threshold of 180 HU within this ROI, thereby triggering the start of the coronary CTA acquisition (^{SURE}Start, Toshiba Medical Systems). The coronary CTA acquisition was optimized for heart rate, patient attenuation (size, weight), and sex [6] (Table 1). A software application (^{SURE}Cardio, Toshiba Medical Systems) selected automatically the optimal pitch [7]. Overranging was taken into account for the helical coronary CTA acquisition [8]; all acquisitions were performed at a tube voltage of 120 kV.

Development of Patient Models

Patient models (voxel phantoms) were constructed from CT scans of the entire trunk of six adult patients (matrix, 256 × 256; voxel height, 3 mm; average pixel size, 1.6 mm^2 [range, 1.5–1.7 mm^2]). Patients who underwent these six CT scans of the trunk were not part of the population that was recruited in the CORE 64 study. The patient models represent three men (Fig. 1, upper row) and three women in three body size categories: small, normal, and obese. Segmentation of organs in the patient models was performed (Fig. 1, middle row). For skin, lung, bone surface, and bone marrow, segmentation was performed automatically with a simple algorithm based on thresholding and contour detection. For the other organs—that is, the adrenals, urinary bladder, breasts, colon, intestine, heart, liver, spleen, kidneys, esophagus, ovaries, pancreas, stomach, thymus, thyroid, uterus, and gallbladder, manual segmentation was performed by x-ray technologists under the supervision of a radiologist. The trunk models developed in this study did not include the extremities or head.

TABLE 1: Selection of Tube Current for the Coronary CT Angiography Examinations

Sex, Weight	Pitch Factor[a]	Tube Current (mA)
Males		
< 60 kg	< 0.225	300
	≥ 0.225	310
60–80 kg	< 0.225	340
	≥ 0.225	360
> 80 kg	< 0.225	360
	≥ 0.225	400
Females		
All weights	< 0.225	240
	≥ 0.225	270

Note—All studies were performed at a tube voltage of 120 kV and in a 64-slice configuration with a 0.5-mm slice thickness.
[a]In the clinical trial, mainly the heart rate–dependent pitch factor of 0.2 or 0.225 was selected.

For the assessment of tissues distributed throughout the entire body—that is, red bone marrow, skin, and bone surface—we assumed that doses outside the trunk area would be zero. A correction was made for the proportion of red bone marrow, skin, and bone surface outside the trunk. The proportion of red bone marrow outside the range of the trunk models was estimated as 17.5% [9]. The proportion of skin outside the

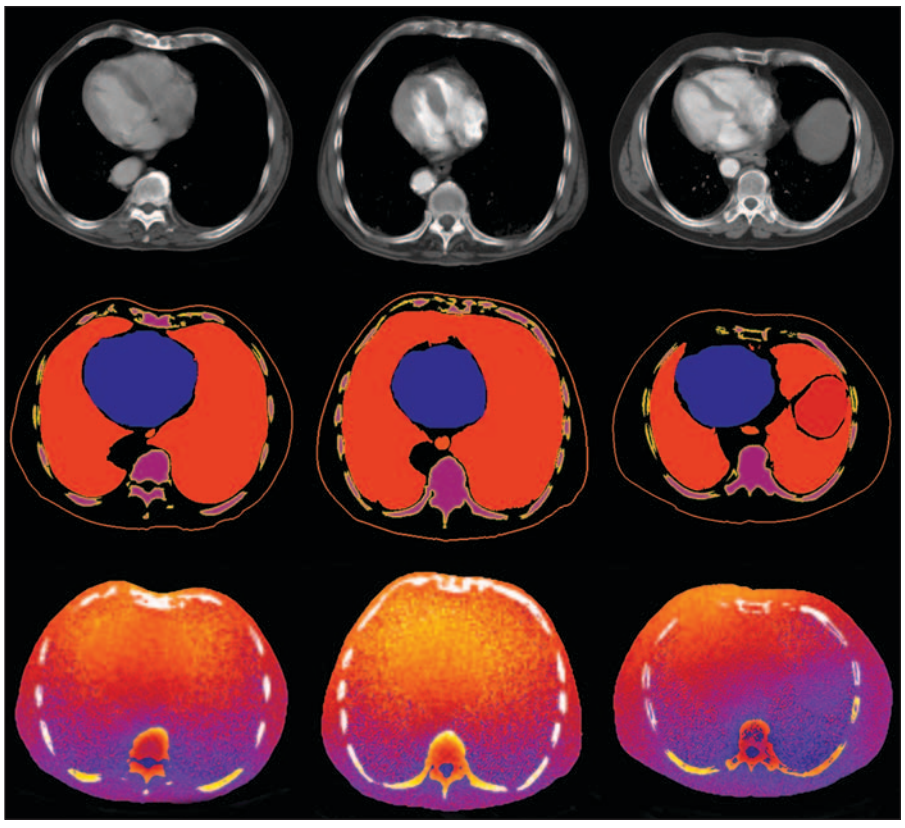

Fig. 1—CT images illustrate physique of males used to create six voxel phantoms (*top row*), organ segmentations (skin, lungs, bone, bone surface, esophagus, *middle row*), and calculated dose distributions (*bottom row*).

TABLE 2: Validation of the Scanner Output as Implemented in the Monte Carlo Simulations by Comparison of Measured Dose Values and Calculated Values as Normalized CT Dose Index 100 ($CTDI_{100}$) Values

Position(s) in the Phantom	Normalized $CTDI_{100}$ Values (mGy/mAs)		Difference Between Simulation and Measurement (%)
	Measured	Monte Carlo Simulation	
North	0.111	0.111	–0.2
East	0.106	0.107	0.6
South	0.088	0.088	–0.1
West	0.112	0.108	–3.7
Center	0.059	0.061	4.0
Average of north, east, south, and west	0.104	0.103	–0.9
Weighted sum of center and average of north, east, south, and west	0.089	0.089	0.2

trunk was derived from the average surface area for different anatomic areas in adults, and it was estimated to be 64%. The proportion of bone surface and muscle tissue outside the range of the trunk was estimated as being equal to that of red bone marrow (i.e., 17.5%).

Monte Carlo Dosimetry

Monte Carlo dosimetry was performed with an algorithm based on the Electron Gamma Shower V4 (EGS4) code [10] in combination with low-energy photon-scattering expansion that was developed by the National Laboratory for High Energy Physics (Japan). Linear (CT scanograms), circular (coronary calcium scoring, ROI planning, bolus tracking), and helical (coronary CTA) pathways of the x-ray tube relative to the patient were modeled. A validation of the EGS4 Monte Carlo algorithm for the Aquilion 64 CT scanner was achieved in this study by comparing measured and calculated values of CT dose index 100 ($CTDI_{100}$) values.

Dosimetry With a CT Ionization Chamber

The output of the CT scanners at all nine hospitals participating in the CORE 64 study was assessed by measuring the normalized $CTDI_{100}$ (mGy/mAs) under standardized conditions by local technicians in a standard cylindric CT dose body phantom. Calibrated 100-mm-long CT ionization chambers were used.

Dose Calculations

The Monte Carlo dose simulation algorithm was used to assess the dose distribution in our six patient models for the acquisition protocol used during the CORE 64 study. The start and end positions of the acquisitions were identified by an x-ray technologist with 6 years of experience in cardiac CT acquisitions. Effective dose was calculated not only according to the recent International Commission on Radiological Protection (ICRP) Report 103 [11], but also according to a previous ICRP publication, Report 60 [12]. For cardiac CT, a significant effect on effective dose assessment could be expected from the increase of the tissue weighting factor for breast tissue in ICRP 103 compared with the tissue weighting factor in ICRP 60.

Different CT acquisition protocols were used for males and females; therefore, sex-specific calculations of effective dose had to be performed. For the calculation of effective dose to males, no tissue weighting factor for the breasts was applied; for females, a tissue weighting factor for breast tissue of, respectively, 0.10 (ICRP 60) and 0.24 (ICRP 103) was used. From the results, sex-averaged effective dose (E) to dose-length product (DLP) conversion factors (E / DLP) were derived for coronary CTA acquisitions [13].

For comparison with the results that we derived for our two normal-sized patient models, effective dose for coronary CTA was also calculated using the ImPACT CT Dosimetry Calculator [14] and using our Monte Carlo algorithm also for four other standard-sized patient models representing standard-sized adult males and females—that is, the Golem and Laura [15] and the Adam and Eve [15, 16] patient models.

Results

Dosimetry With CT Ionization Chambers

The normalized weighted $CTDI_{100}$ ($CTDI_{100,w}$) for coronary CTA acquisitions at the nine participating centers was, on average, 0.086 mGy/mAs (SD, 6%; range, 0.080–0.094 mGy/mAs). The good agreement between sites confirms that variation in radiation output was only minimal between the nine different CT scanners that were installed at the centers participating in the CORE 64 study. For the coronary CTA acquisitions in the clinical trial, we derived an average volume $CTDI_{100}$ ($CTDI_{100,vol}$) of 41 mGy for women and $CTDI_{100,vol}$ of 52, 59, and 62 mGy for, respectively, the small, normal-sized, and obese men (pitch factor, 0.2). We derived the DLP from the measured $CTDI_{100,w}$, the pitch factor, and the exposed range. The DLP for coronary CTA acquisitions including overranging was, respectively, 635, 476, and 556 mGy · cm for the small, normal-sized, and obese female models and 761, 862, and 794 mGy · cm, respectively, for the male models.

Dose Calculations

Excellent agreement between measured and simulated $CTDI_{100}$ values—that is, within a range of ± 4%—was found (Table 2). This result confirms that dose calculations obtained using our Monte Carlo algorithm accurately simulate actual exposure conditions.

Figure 2 provides an overview of selected organ doses for coronary CTA (pitch factor, 0.2); doses to only the seven organs that contribute most to effective dose according to ICRP 103 are presented. The highest average equivalent organ doses for our normal-sized patient models were observed for, respectively, breast tissue, 38 mSv; lung, 35 mSv; liver, 32 mSv; stomach, 29 mSv; and esophagus, 27 mSv. The largest contributors to effective dose were breast tissue in women and lungs and stomach in men and women. Red bone marrow and the thyroid also received a considerable dose. Exposure of organs located a greater distance from the examined region were much lower: For example, dose to the bladder was 0.2 mSv or less; to the ovaries, 0.2 mSv or less; and to the testes, 0.02 mSv or less. Considerable variation in organ doses was observed between the different patient models.

Effective dose is reported according to the ICRP 103 definition and to the previous ICRP 60 here and in Table 3. Table 3 lists the size-specific, sex-averaged effective doses for all acquisitions of the cardiac CT protocol. The main contribution to the sex-averaged effective dose resulted from the coronary CTA acquisition. A smaller but not negligible contribution to effective dose re-

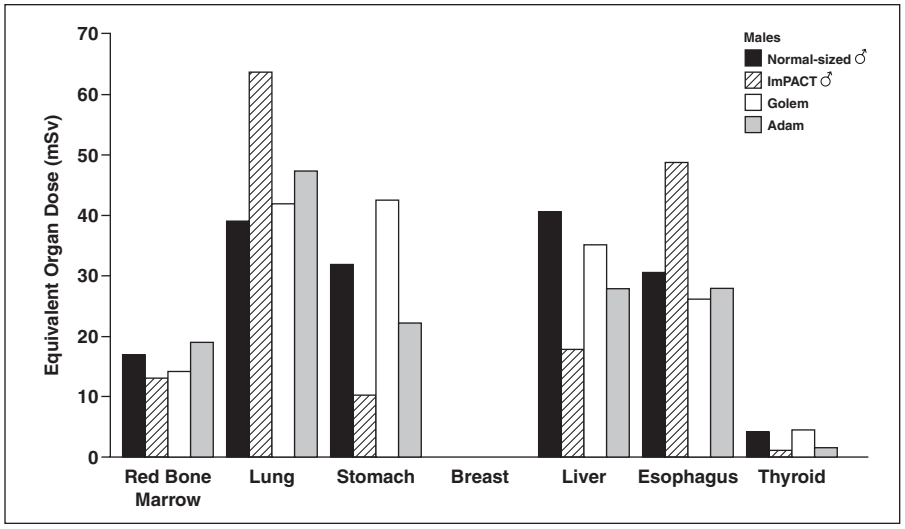

A

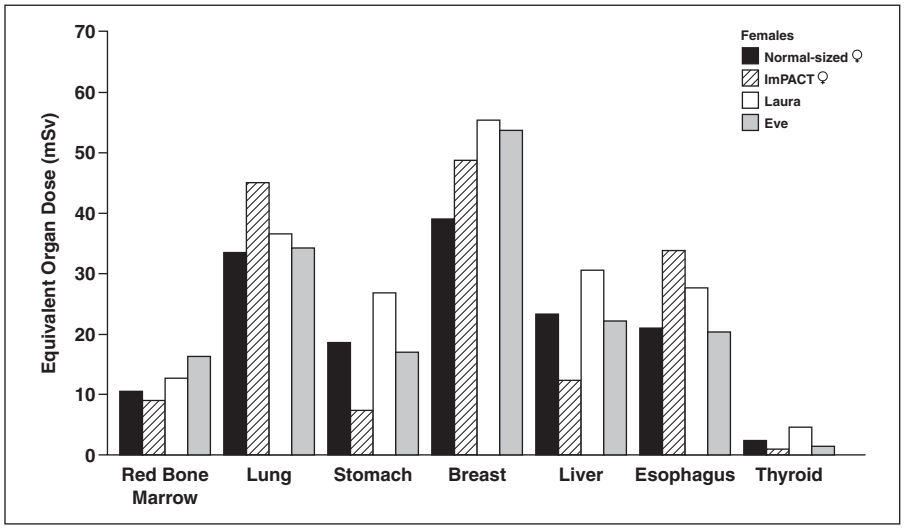

B

Fig. 2—Equivalent dose (mGy) for seven organs that contribute most to effective dose according to Report 103 [11] of the International Commission on Radiological Protection (ICRP).
A and **B,** Organ doses are presented for ECG-gated coronary CT angiography acquisitions, and they are calculated for different normal-sized patient models. All calculations were performed for pitch factor of 0.2 and tube voltage of 120 kV. Calculations for ImPACT phantoms were performed with ImPACT CT Dosimetry Calculator. All other calculations presented in this article were performed using Monte Carlo dosimetry simulation algorithm. Note that acquisition protocols were different for men (**A**) and women (**B**) (see Table 1).

sulted from coronary calcium scoring, ranging between 1.7 and 2.6 mSv according to ICRP 103 and between 1.4 and 2.0 mSv according to ICRP 60. Contributions of CT scanograms, ROI planning, and bolus tracking were very small (≤ 0.3 mSv).

Figure 3 shows an overview of the calculated effective doses for coronary CTA acquisitions for standard-sized adults and for one anthropomorphic mathematic phantom (ImPACT CT Patient Dosimetry Calculator, version 1.0.3); for two sex-specific mathematic phantoms (Adam and Eve); and for four sex-specific voxel phantoms (the two phantoms developed in this study and the Golem and Laura phantoms). Compared with organ dose assessment, there is better agreement in the calculated effective dose values for the different standard-sized patient models.

Using ICRP 103, we calculated for coronary CTA a sex-averaged conversion factor for the calculation of effective dose from a DLP of 0.030 mSv/mGy · cm (range, 0.019–0.043 mSv/mGy · cm). Using ICRP 60, we calculated for coronary CTA a sex-averaged conversion factor for the calculation of effective dose from a DLP of 0.024 mSv/mGy · cm (range, 0.017–0.030 mSv/mGy · cm). Because published effective doses for coronary CTA are often traceable to conversion factors derived from the ImPACT CT Dosimetry Calculator, an effective dose conversion factor was also derived for the ImPACT CT Dosimetry Calculator, yielding a value of 0.026 mSv/mGy · cm according to ICRP 103 and 0.020 mSv/mGy · cm according to ICRP 60.

Discussion

We accomplished our aim to accurately assess radiation exposure associated with the cardiac CT acquisition protocol of the CORE 64 study after developing an algorithm for Monte Carlo dosimetry adapted to the characteristics of the Aquilion 64 CT scanner and after developing six patient models representing men and women of different physiques. Substantial efforts were invested in developing the dosimetric methodology because current methods for assessment of patient dose are not well suited for cardiac CT acquisitions for various reasons: They apply only to normal-sized mathematic patient models; they are based on old types of axial CT scanners; they assume positioning of the patient in the center of rotation of the scanner; and they do not allow assessment of patient dose from CT scanograms.

Patient sex-averaged and size-averaged effective dose values based on definitions from ICRP 103 were assessed to be, respectively, 19 mSv for only coronary CTA and 22 mSv for the full cardiac CT acquisition protocol, including two CT scanograms, calcium scoring, ROI planning, bolus tracking, and coronary CTA. The sex-averaged effective dose was 16 mSv and size-averaged dose was 18 mSv using definitions from ICRP. We recommend use of an *E* / *DLP* dose conversion factor of 0.030 mSv/mGy · cm for cardiac CT (ICRP 103). Although many studies have reported on patient exposures resulting from coronary CTA, this study is, to our knowledge, the first study that applied a dosimetric methodology that is well adapted to a modern CT scanner and to a patient size-specific and sex-specific cardiac CT acquisition protocol.

In this study effective dose was calculated according to the recent ICRP 103 publication and to the ICRP 60 publication. The reasons for presenting effective dose values also according to the ICRP 60 definition were, first, that the CORE 64 multicenter study was pre-

TABLE 3: Sex-Averaged Effective Doses for Cardiac CT Examinations[a] Calculated for Six Voxel Phantoms With Electron Gamma Shower V4 (EGS4) Monte Carlo Dosimetry and Averaged for Sex

Examination	Sex-Averaged Effective Dose (mSv) According to ICRP 103 [According to ICRP 60]		
	Normal-Sized Patient	Obese Patient	Small Patient
Coronary CT angiography			
Pitch factor of 0.2	18.3 [14.7]	17.2 [14.4]	22.2 [18.1]
Pitch factor of 0.225	17.9 [14.3]	17.1 [14.3]	21.4 [17.4]
CT scanogram			
Lateral	0.04 [0.04]	0.04 [0.03]	0.05 [0.04]
Frontal	0.1 [0.08]	0.09 [0.07]	0.12 [0.10]
Coronary calcium scoring	2.1 [1.6]	1.7 [1.4]	2.6 [2.0]
Region-of-interest planning	0.006 [0.005]	0.006 [0.005]	0.011 [0.007]
Bolus tracking	0.1 [0.1]	0.2 [0.1]	0.3 [0.2]
Total			
Pitch factor of 0.2	20.7 [16.6]	19.2 [16.0]	25.2 [20.5]
Pitch factor of 0.225	20.2 [16.2]	19.1 [15.9]	24.5 [19.8]

Note—ICRP 103 = Report 103 of the International Commission on Radiological Protection (ICRP) [11], ICRP 60 = Report 60 of the ICRP [12].
[a]The multicenter Coronary Artery Evaluation Using 64-Row Multidetector Computed Tomography Angiography (CORE 64) trial [3].

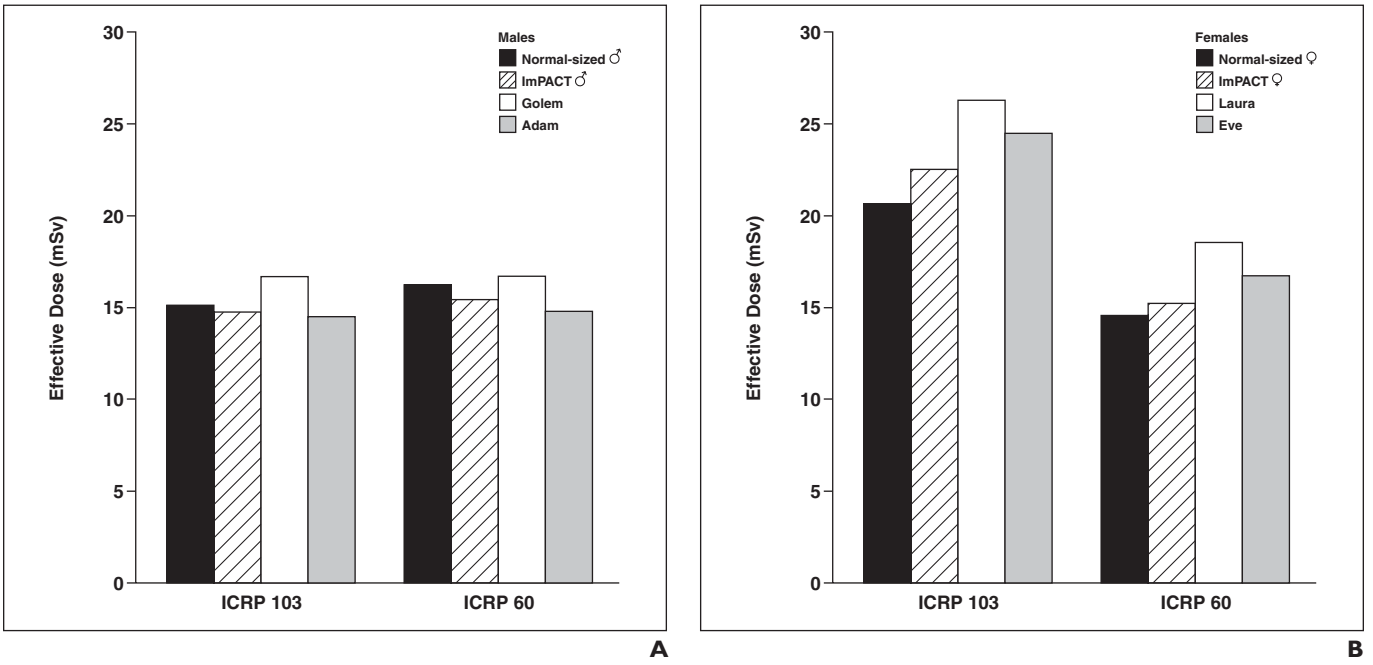

Fig. 3—Comparison of effective dose (mSv) according to Reports 103 [11] and 60 [12] of the International Commission on Radiological Protection (ICRP) for coronary CT angiography (CTA) calculated for different phantoms.
A and **B,** All calculations were performed for pitch factor of 0.2 and tube voltage of 120 kV. Calculations for ImPACT phantoms were performed with ImPACT CT Dosimetry Calculator. All other calculations presented in this article were performed using Monte Carlo dosimetry simulation algorithm. Note that acquisition protocols were different for men (**A**) and women (**B**) (see Table 1).

pared before ICRP 103 was published, so all considerations on effective dose with regard to the CORE 64 study were based on ICRP 60 (e.g., acquisition protocol development and medical ethical aspects); and, second, that the substantial body of published literature on effective dose in cardiac CT is still based on the definition of effective dose in ICRP 60. Effective dose becomes much higher for cardiac CT when assessed according to the now preferred ICRP 103 publication because of the higher weighting factor for breast tissue. Sex-averaged effective dose is estimated to be about 25% higher with the application of ICRP 103 compared with ICRP 60. Effective doses for the different standard-sized patient models are in rather good agreement (Fig. 3), whereas relatively large variations in organ dose were observed between the same patient models (Fig. 2). This indicates that assessment of effective dose is rather insensitive for

the choice of a specific patient model; however, accurate assessment of organ dose is much more complicated.

Many groups have reported on effective dose for coronary CTA with 2 × 32, 64, and 320 detector-row scanners including 2 × 32 detector-row dual-source scanners. Forty-nine reported values of effective dose were found in 31 different studies. Analysis of these values however raised concern with regard to the accuracy of many of the reported effective doses. First, from the total of 49 reported dose values, only nine values (from four studies) were traceable to actual dose measurements [17–20]; for 10 values (from nine studies), it remained unclear if dose measurements were performed or if the dose indication on the scanner was calibrated appropriately [1, 21–28]. Many of the reported dose values—that is, 30 of the 49 reported dose values—were not traceable to dose measurements; in these cases, the effective dose was derived from the DLP or CTDI as indicated on the operator's console. In scientific studies, it would be preferable that reported dose values are at least traceable to an actual dose measurement. Second, the methodology for calculating effective dose was not appropriate in many of the studies. In five studies, investigators did not mention how they calculated effective doses, which is a major shortcoming [21, 22, 24, 26, 28].

The method applied most often for effective dose assessment (28 reported values, 16 studies) was based on the *E* / *DLP* conversion factor of 0.017 mSv/mGy · cm that is derived for general chest CT [18, 20, 29–42]. According to our study, this method is not appropriate and yields an underestimation of effective dose of 43% if ICRP 103 is used or 29% if ICRP 60 is used. One study used an even lower conversion factor of 0.014 mSv/Gy [43]; that conversion factor, compared with our results, could lead to an underestimation of effective dose of 53% (ICRP 103) or 42% (ICRP 60). The reason that an *E* / *DLP* conversion factor derived for general chest CT yields systematic and substantial underestimation of effective dose in cardiac CT is that the *E* / *DLP* conversion factor has been published as a rough estimate for a regular CT acquisition of the entire chest. In cardiac CT, in contrast to general chest CT, the acquisition is limited to a small part of the chest. This part is relatively sensitive for radiation exposure because it includes the female breast tissue. The effective dose conversion factors that we derived from the IMPACT CT Dosimetry Calculator (ICRP 103 and ICRP 60: 0.026 and 0.020 mSv/mGy · cm, respectively) confirm that it is not appropriate to use 0.017 and 0.014 mSv/mGy · cm as *E* / *DLP* conversion factors.

For helical acquisition and retrospective ECG-gated reconstruction, the reported dose values corresponded to an average effective dose of 15 mSv (range, 8.6–18 mSv; 13 reported effective dose values) [1, 17, 23, 25, 27, 29, 31, 44–46]; for a helical acquisition with ECG-triggered modulation of tube current and retrospective ECG-gated reconstruction, to an average effective dose of 12 mSv (range, 4–21 mSv; 18 reported effective dose values) [21–24, 26, 30–33, 35–38, 41, 47]; for helical acquisition of a small phantom (55-kg adult) and retrospective ECG-gated reconstruction, to 22 mSv (range, 12–32 mSv; five reported effective dose values) [18, 19]; for a step-and-shoot prospective ECG-triggered acquisition, to an average effective dose of 4 mSv (range, 1.2–6.7 mSv; 12 reported effective dose values) [20, 29, 32, 34, 37, 39, 40, 42]; and, finally, for an extensive field survey including 50 participating sites, to an average effective dose of 12 mSv [43]. The exceptional high effective doses of 28 and 32 mSv were reported in studies that used thermoluminescence dosimetry and a rather small anthropomorphic phantom [18, 19]; the reason for those high effective doses is probably that the CT acquisition was not properly adapted to the small size of the phantom.

Our effective dose for the normal-sized patient model of 15 mSv (Table 3, ICRP 60 definition) is equal to the reported average effective dose (15 mSv; range, 8.6–18 mSv) for helical acquisition and retrospective ECG-gated reconstruction. The published values show a trend of substantial dose reduction when a helical acquisition with tube current modulation is used (12 mSv) and even more when prospectively triggered axial step-and-shoot acquisitions are used (4 mSv). This observation suggests that with the wider implementation of these dose-saving acquisition techniques, patient dose in cardiac CT decreases substantially. New technologies that allow scanning the entire heart within one heartbeat now have become available and are expected to contribute to further optimization of cardiac CT examinations. Such acquisitions can be achieved with high-pitch dual-source CT [48] and volumetric CT [49, 50]. These technologies are expected to provide opportunities for optimization of cardiac CT, with regard to both better image quality and much reduced patient dose. Further research needs to address if and to what extent these expectations can be realized.

References

1. Dewey M, Hoffmann H, Hamm B. CT coronary angiography using 16 and 64 simultaneous detector rows: intraindividual comparison. *Rofo* 2007; 179:581–586
2. Hausleiter J, Meyer T, Hadamitzky M, et al. Noninvasive coronary computed tomographic angiography for patients with suspected coronary artery disease: the Coronary Angiography by Computed Tomography with the Use of a Submillimeter resolution (CACTUS) trial. *Eur Heart J* 2007; 28: 3034–3041
3. Miller JM, Rochitte CE, Dewey M, et al. Diagnostic performance of coronary angiography by 64-row CT. *N Engl J Med* 2008; 359:2324–2336
4. Dewey M, Teige F, Schnapauff D, et al. Noninvasive detection of coronary artery stenoses with multislice computed tomography or magnetic resonance imaging. *Ann Intern Med* 2006; 145: 407–415
5. Meijboom WB, van Mieghem CA, Mollet NR, et al. 64-slice computed tomography coronary angiography in patients with high, intermediate, or low pretest probability of significant coronary artery disease. *J Am Coll Cardiol* 2007; 50:1469–1475
6. Miller JM, Dewey M, Vavere AL, et al. Coronary CT angiography using 64 detector rows: methods and design of the multi-centre trial CORE-64. *Eur Radiol* 2009; 19:816–828
7. Engelken FJ, Lembcke A, Hamm B, Dewey M. Determining optimal acquisition parameters for computed tomography coronary angiography: evaluation of a software-assisted, breathhold exam simulation. *Acad Radiol* 2009; 16:239–243
8. van der Molen AJ, Geleijns J. Overranging in multisection CT: quantification and relative contribution to dose—comparison of four 16-section CT scanners. *Radiology* 2007; 242:208–216
9. Cristy M. Active bone marrow distribution as a function of age in humans. *Phys Med Biol* 1981; 26:389–400
10. Nelson WR, Hirayama H, Rogers DWO. The EGS code system. Menlo Park, CA: SLAC National Linear Accelerator Center, 1985: Report no.: SLAC-265
11. International Commission on Radiological Protection. The 2007 Recommendations of the International Commission on Radiological Protection. Bethesda, MD: ICRP, 2007: Publication no. 103
12. International Commission on Radiological Protection. The 1990 recommendations of the International Commission on Radiological Protection. Bethesda, MD: ICRP, 1991: Publication no. 60

13. Huda W, Ogden KM, Khorasani MR. Converting dose-length product to effective dose at CT. *Radiology* 2008; 248:995–1003
14. Shrimpton PC, Edyvean S. CT scanner dosimetry. *Br J Radiol* 1998; 71:1–3
15. Zankl M, Wittmann A. The adult male voxel model "Golem" segmented from whole-body CT patient data. *Radiat Environ Biophys* 2001; 40:153–162
16. Jacob P, Paretzke HG, Rosenbaum H, Zankl M. Organ doses from radionuclides on the ground. Part I. Simple time dependences. *Health Phys* 1988; 54:617–633
17. Francone M, Di CE, Napoli A, et al. Dose reduction and image quality assessment in 64-detector row computed tomography of the coronary arteries using an automatic exposure control system. *J Comput Assist Tomogr* 2008; 32:668–678
18. Hurwitz LM, Reiman RE, Yoshizumi TT, et al. Radiation dose from contemporary cardiothoracic multidetector CT protocols with an anthropomorphic female phantom: implications for cancer induction. *Radiology* 2007; 245:742–750
19. Mori S, Nishizawa K, Kondo C, Ohno M, Akahane K, Endo M. Effective doses in subjects undergoing computed tomography cardiac imaging with the 256-multislice CT scanner. *Eur J Radiol* 2008; 65:442–448
20. Rybicki FJ, Otero HJ, Steigner ML, et al. Initial evaluation of coronary images from 320-detector row computed tomography. *Int J Cardiovasc Imaging* 2008; 24:535–546
21. Caussin C, Larchez C, Ghostine S, et al. Comparison of coronary minimal lumen area quantification by sixty-four-slice computed tomography versus intravascular ultrasound for intermediate stenosis. *Am J Cardiol* 2006; 98:871–876
22. Delhaye D, Remy-Jardin M, Rozel C, et al. Coronary artery imaging during preoperative CT staging: preliminary experience with 64-slice multidetector CT in 99 consecutive patients. *Eur Radiol* 2007; 17:591–602
23. Einstein AJ, Henzlova MJ, Rajagopalan S. Estimating risk of cancer associated with radiation exposure from 64-slice computed tomography coronary angiography. *JAMA* 2007; 298:317–323
24. Leber AW, Knez A, von Ziegler F, et al. Quantification of obstructive and nonobstructive coronary lesions by 64-slice computed tomography: a comparative study with quantitative coronary angiography and intravascular ultrasound. *J Am Coll Cardiol* 2005; 46:147–154
25. Mollet NR, Cademartiri F, van Mieghem CA, et al. High-resolution spiral computed tomography coronary angiography in patients referred for diagnostic conventional coronary angiography. *Circulation* 2005; 112:2318–2323
26. Nikolaou K, Knez A, Rist C, et al. Accuracy of 64-MDCT in the diagnosis of ischemic heart disease. *AJR* 2006; 187:111–117
27. Pugliese F, Mollet NR, Runza G, et al. Diagnostic accuracy of non-invasive 64-slice CT coronary angiography in patients with stable angina pectoris. *Eur Radiol* 2006; 16:575–582
28. Raff GL, Gallagher MJ, O'Neill WW, Goldstein JA. Diagnostic accuracy of noninvasive coronary angiography using 64-slice spiral computed tomography. *J Am Coll Cardiol* 2005; 46:552–557
29. Earls JP, Schrack EC. Prospectively gated low-dose CCTA: 24 months experience in more than 2,000 clinical cases. *Int J Cardiovasc Imaging* 2009; 25:177–187
30. Ghostine S, Caussin C, Daoud B, et al. Non-invasive detection of coronary artery disease in patients with left bundle branch block using 64-slice computed tomography. *J Am Coll Cardiol* 2006; 48:1929–1934
31. Hausleiter J, Meyer T, Hadamitzky M, et al. Radiation dose estimates from cardiac multislice computed tomography in daily practice: impact of different scanning protocols on effective dose estimates. *Circulation* 2006; 113:1305–1310
32. Hirai N, Horiguchi J, Fujioka C, et al. Prospective versus retrospective ECG-gated 64-detector coronary CT angiography: assessment of image quality, stenosis, and radiation dose. *Radiology* 2008; 248:424–430
33. Husmann L, Herzog BA, Gaemperli O, et al. Diagnostic accuracy of computed tomography coronary angiography and evaluation of stress-only single-photon emission computed tomography/computed tomography hybrid imaging: comparison of prospective electrocardiogram-triggering vs. retrospective gating. *Eur Heart J* 2009; 30:600–607
34. Husmann L, Valenta I, Gaemperli O, et al. Feasibility of low-dose coronary CT angiography: first experience with prospective ECG-gating. *Eur Heart J* 2008; 29:191–197
35. Leschka S, Stolzmann P, Schmid FT, et al. Low kilovoltage cardiac dual-source CT: attenuation, noise, and radiation dose. *Eur Radiol* 2008; 18: 1809–1817
36. Leschka S, Alkadhi H, Stolzmann P, et al. Monoversus bisegment reconstruction algorithms for dual-source computed tomography coronary angiography. *Invest Radiol* 2008; 43:703–711
37. Maruyama T, Takada M, Hasuike T, Yoshikawa A, Namimatsu E, Yoshizumi T. Radiation dose reduction and coronary assessability of prospective electrocardiogram-gated computed tomography coronary angiography: comparison with retrospective electrocardiogram-gated helical scan. *J Am Coll Cardiol* 2008; 52:1450–1455
38. Paul JF, Abada HT. Strategies for reduction of radiation dose in cardiac multislice CT. *Eur Radiol* 2007; 17:2028–2037
39. Scheffel H, Alkadhi H, Leschka S, et al. Low-dose CT coronary angiography in the step-and-shoot mode: diagnostic performance. *Heart* 2008; 94:1132–1137
40. Stolzmann P, Scheffel H, Leschka S, et al. Influence of calcifications on diagnostic accuracy of coronary CT angiography using prospective ECG triggering. *AJR* 2008; 191:1684–1689
41. Stolzmann P, Scheffel H, Schertler T, et al. Radiation dose estimates in dual-source computed tomography coronary angiography. *Eur Radiol* 2008; 18:592–599
42. Stolzmann P, Leschka S, Scheffel H, et al. Dual-source CT in step-and-shoot mode: noninvasive coronary angiography with low radiation dose. *Radiology* 2008; 249:71–80
43. Hausleiter J, Meyer T, Hermann F, et al. Estimated radiation dose associated with cardiac CT angiography. *JAMA* 2009; 301:500–507
44. Francone M, Napoli A, Carbone I, et al. Noninvasive imaging of the coronary arteries using a 64-row multidetector CT scanner: initial clinical experience and radiation dose concerns. *Radiol Med* 2007; 112:31–46
45. Muhlenbruch G, Seyfarth T, Soo CS, Pregalathan N, Mahnken AH. Diagnostic value of 64-slice multi-detector row cardiac CTA in symptomatic patients. *Eur Radiol* 2007; 17:603–609
46. Raff GL, Goldstein JA. Coronary angiography by computed tomography: coronary imaging evolves. *J Am Coll Cardiol* 2007; 49:1830–1833
47. Weustink AC, Mollet NR, Pugliese F, et al. Optimal electrocardiographic pulsing windows and heart rate: effect on image quality and radiation exposure at dual-source coronary CT angiography. *Radiology* 2008; 248:792–798
48. Goetti R, Feuchtner G, Stolzmann P, et al. High-pitch dual-source CT coronary angiography: systolic data acquisition at high heart rates. *Eur Radiol* 2010; 20:2565–2571
49. Dewey M, Zimmermann E, Deissenrieder F, et al. Noninvasive coronary angiography by 320-row computed tomography with lower radiation exposure and maintained diagnostic accuracy: comparison of results with cardiac catheterization in a head-to-head pilot investigation. *Circulation* 2009; 120:867–875
50. Dewey M, Zimmermann E, Laule M, Rutsch W, Hamm B. Three-vessel coronary artery disease examined with 320-slice computed tomography coronary angiography. *Eur Heart J* 2008; 29:1669